The Ratio of Jet Cross Sections at $\sqrt{s} = 630$ GeV and 1800 GeV

B. Abbott,[50] M. Abolins,[47] V. Abramov,[23] B.S. Acharya,[15] D.L. Adams,[57] M. Adams,[34] G.A. Alves,[2] N. Amos,[46] E.W. Anderson,[39] M.M. Baarmand,[52] V.V. Babintsev,[23] L. Babukhadia,[52] A. Baden,[43] B. Baldin,[33] P.W. Balm,[18] S. Banerjee,[15] J. Bantly,[56] E. Barberis,[26] P. Baringer,[40] J.F. Bartlett,[33] U. Bassler,[11] A. Bean,[40] M. Begel,[51] A. Belyaev,[22] S.B. Beri,[13] G. Bernardi,[11] I. Bertram,[24] A. Besson,[9] V.A. Bezzubov,[23] P.C. Bhat,[33] V. Bhatnagar,[13] M. Bhattacharjee,[52] G. Blazey,[35] S. Blessing,[31] A. Boehnlein,[33] N.I. Bojko,[23] F. Borcherding,[33] A. Brandt,[57] R. Breedon,[27] G. Briskin,[56] R. Brock,[47] G. Brooijmans,[33] A. Bross,[33] D. Buchholz,[36] M. Buehler,[34] V. Buescher,[51] V.S. Burtovoi,[23] J.M. Butler,[44] F. Canelli,[51] W. Carvalho,[3] D. Casey,[47] Z. Casilum,[52] H. Castilla-Valdez,[17] D. Chakraborty,[52] K.M. Chan,[51] S.V. Chekulaev,[23] D.K. Cho,[51] S. Choi,[30] S. Chopra,[53] J.H. Christenson,[33] M. Chung,[34] D. Claes,[48] A.R. Clark,[26] J. Cochran,[30] L. Coney,[38] B. Connolly,[31] W.E. Cooper,[33] D. Coppage,[40] M.A.C. Cummings,[35] D. Cutts,[56] O.I. Dahl,[26] G.A. Davis,[51] K. Davis,[25] K. De,[57] K. Del Signore,[46] M. Demarteau,[33] R. Demina,[41] P. Demine,[9] D. Denisov,[33] S.P. Denisov,[23] S. Desai,[52] H.T. Diehl,[33] M. Diesburg,[33] G. Di Loreto,[47] S. Doulas,[45] P. Draper,[57] Y. Ducros,[12] L.V. Dudko,[22] S. Duensing,[19] S.R. Dugad,[15] A. Dyshkant,[23] D. Edmunds,[47] J. Ellison,[30] V.D. Elvira,[33] R. Engelmann,[52] S. Eno,[43] G. Eppley,[59] P. Ermolov,[22] O.V. Eroshin,[23] J. Estrada,[51] H. Evans,[49] V.N. Evdokimov,[23] T. Fahland,[29] S. Feher,[33] D. Fein,[25] T. Ferbel,[51] H.E. Fisk,[33] Y. Fisyak,[53] E. Flattum,[33] F. Fleuret,[26] M. Fortner,[35] K.C. Frame,[47] S. Fuess,[33] E. Gallas,[33] A.N. Galyaev,[23] P. Gartung,[30] V. Gavrilov,[21] R.J. Genik II,[24] K. Genser,[33] C.E. Gerber,[34] Y. Gershtein,[56] B. Gibbard,[53] R. Gilmartin,[31] G. Ginther,[51] B. Gómez,[5] G. Gómez,[43] P.I. Goncharov,[23] J.L. González Solís,[17] H. Gordon,[53] L.T. Goss,[58] K. Gounder,[30] A. Goussiou,[52] N. Graf,[53] G. Graham,[43] P.D. Grannis,[52] J.A. Green,[39] H. Greenlee,[33] S. Grinstein,[1] L. Groer,[49] P. Grudberg,[26] S. Grünendahl,[33] A. Gupta,[15] S.N. Gurzhiev,[23] G. Gutierrez,[33] P. Gutierrez,[55] N.J. Hadley,[43] H. Haggerty,[33] S. Hagopian,[31] V. Hagopian,[31] K.S. Hahn,[51] R.E. Hall,[28] P. Hanlet,[45] S. Hansen,[33] J.M. Hauptman,[39] C. Hays,[49] C. Hebert,[40] D. Hedin,[35] A.P. Heinson,[30] U. Heintz,[44] T. Heuring,[31] R. Hirosky,[34] J.D. Hobbs,[52] B. Hoeneisen,[8] J.S. Hoftun,[56] S. Hou,[46] Y. Huang,[46] A.S. Ito,[33] S.A. Jerger,[47] R. Jesik,[37] K. Johns,[25] M. Johnson,[33] A. Jonckheere,[33] M. Jones,[32] H. Jöstlein,[33] A. Juste,[33] S. Kahn,[53] E. Kajfasz,[10] D. Karmanov,[22] D. Karmgard,[38] R. Kehoe,[38] S.K. Kim,[16] B. Klima,[33] C. Klopfenstein,[27] B. Knuteson,[26] W. Ko,[27] J.M. Kohli,[13] A.V. Kostritskiy,[23] J. Kotcher,[53] A.V. Kotwal,[49] A.V. Kozelov,[23] E.A. Kozlovsky,[23] J. Krane,[39] M.R. Krishnaswamy,[15] S. Krzywdzinski,[33] M. Kubantsev,[41] S. Kuleshov,[21] Y. Kulik,[52] S. Kunori,[43] V.E. Kuznetsov,[30] G. Landsberg,[56] A. Leflat,[22] F. Lehner,[33] J. Li,[57] Q.Z. Li,[33] J.G.R. Lima,[3] D. Lincoln,[33] S.L. Linn,[31] J. Linnemann,[47] R. Lipton,[33] A. Lucotte,[52] L. Lueking,[33] C. Lundstedt,[48] A.K.A. Maciel,[35] R.J. Madaras,[26] V. Manankov,[22] H.S. Mao,[4] T. Marshall,[37] M.I. Martin,[33] R.D. Martin,[34] K.M. Mauritz,[39] B. May,[36] A.A. Mayorov,[37] R. McCarthy,[52] J. McDonald,[31] T. McMahon,[54] H.L. Melanson,[33] X.C. Meng,[4] M. Merkin,[22] K.W. Merritt,[33] C. Miao,[56] H. Miettinen,[59] D. Mihalcea,[55] A. Mincer,[50] C.S. Mishra,[33] N. Mokhov,[33] N.K. Mondal,[15] H.E. Montgomery,[33] R.W. Moore,[47] M. Mostafa,[1] H. da Motta,[2] E. Nagy,[10] F. Nang,[25] M. Narain,[44] V.S. Narasimham,[15] H.A. Neal,[46] J.P. Negret,[5] S. Negroni,[10] D. Norman,[58] L. Oesch,[46] V. Oguri,[3] B. Olivier,[11] N. Oshima,[33] P. Padley,[59] L.J. Pan,[36] A. Para,[33] N. Parashar,[45] R. Partridge,[56] N. Parua,[9] M. Paterno,[51] A. Patwa,[52] B. Pawlik,[20] J. Perkins,[57] M. Peters,[32] O. Peters,[18] R. Piegaia,[1] H. Piekarz,[31] B.G. Pope,[47] E. Popkov,[38] H.B. Prosper,[31] S. Protopopescu,[53] J. Qian,[46] P.Z. Quintas,[33] R. Raja,[33] S. Rajagopalan,[53] E. Ramberg,[33] P.A. Rapidis,[33] N.W. Reay,[41] S. Reucroft,[45] J. Rha,[30] M. Rijssenbeek,[52] T. Rockwell,[47] M. Roco,[33] P. Rubinov,[33] R. Ruchti,[38] J. Rutherfoord,[25] A. Santoro,[2] L. Sawyer,[42] R.D. Schamberger,[52] H. Schellman,[36] A. Schwartzman,[1] J. Sculli,[50] N. Sen,[59] E. Shabalina,[22] H.C. Shankar,[15] R.K. Shivpuri,[14] D. Shpakov,[52] M. Shupe,[25] R.A. Sidwell,[41] V. Simak,[7] H. Singh,[30] J.B. Singh,[13] V. Sirotenko,[33] P. Slattery,[51] E. Smith,[55] R.P. Smith,[33] R. Snihur,[36] G.R. Snow,[48] J. Snow,[54] S. Snyder,[53] J. Solomon,[34] V. Sorín,[1] M. Sosebee,[57] N. Sotnikova,[22] K. Soustruznik,[6] M. Souza,[2] N.R. Stanton,[41] G. Steinbrück,[49] R.W. Stephens,[57] M.L. Stevenson,[26] F. Stichelbaut,[53] D. Stoker,[29] V. Stolin,[21] D.A. Stoyanova,[23] M. Strauss,[55] K. Streets,[50] M. Strovink,[26] L. Stutte,[33] A. Sznajder,[3] W. Taylor,[52] S. Tentindo-Repond,[31] J. Thompson,[43] D. Toback,[43] S.M. Tripathi,[27] T.G. Trippe,[26] A.S. Turcot,[53] P.M. Tuts,[49] P. van Gemmeren,[33] V. Vaniev,[23] R. Van Kooten,[37] N. Varelas,[34] A.A. Volkov,[23] A.P. Vorobiev,[23] H.D. Wahl,[31] H. Wang,[36] Z.-M. Wang,[52] J. Warchol,[38] G. Watts,[60] M. Wayne,[38] H. Weerts,[47] A. White,[57] J.T. White,[58] D. Whiteson,[26] J.A. Wightman,[39] D.A. Wijngaarden,[19] S. Willis,[35] S.J. Wimpenny,[30] J.V.D. Wirjawan,[58] J. Womersley,[33] D.R. Wood,[45] R. Yamada,[33] P. Yamin,[53] T. Yasuda,[33] K. Yip,[33] S. Youssef,[31] J. Yu,[33] Z. Yu,[36] M. Zanabria,[5] H. Zheng,[38] Z. Zhou,[39] Z.H. Zhu,[51] M. Zielinski,[51] D. Zieminska,[37] A. Zieminski,[37] V. Zutshi,[51] E.G. Zverev,[22] and A. Zylberstejn[12]

(DØ Collaboration)

[1] *Universidad de Buenos Aires, Buenos Aires, Argentina*

[2]LAFEX, Centro Brasileiro de Pesquisas Físicas, Rio de Janeiro, Brazil
[3]Universidade do Estado do Rio de Janeiro, Rio de Janeiro, Brazil
[4]Institute of High Energy Physics, Beijing, People's Republic of China
[5]Universidad de los Andes, Bogotá, Colombia
[6]Charles University, Prague, Czech Republic
[7]Institute of Physics, Academy of Sciences, Prague, Czech Republic
[8]Universidad San Francisco de Quito, Quito, Ecuador
[9]Institut des Sciences Nucléaires, IN2P3-CNRS, Universite de Grenoble 1, Grenoble, France
[10]CPPM, IN2P3-CNRS, Université de la Méditerranée, Marseille, France
[11]LPNHE, Universités Paris VI and VII, IN2P3-CNRS, Paris, France
[12]DAPNIA/Service de Physique des Particules, CEA, Saclay, France
[13]Panjab University, Chandigarh, India
[14]Delhi University, Delhi, India
[15]Tata Institute of Fundamental Research, Mumbai, India
[16]Seoul National University, Seoul, Korea
[17]CINVESTAV, Mexico City, Mexico
[18]FOM-Institute NIKHEF and University of Amsterdam/NIKHEF, Amsterdam, The Netherlands
[19]University of Nijmegen/NIKHEF, Nijmegen, The Netherlands
[20]Institute of Nuclear Physics, Kraków, Poland
[21]Institute for Theoretical and Experimental Physics, Moscow, Russia
[22]Moscow State University, Moscow, Russia
[23]Institute for High Energy Physics, Protvino, Russia
[24]Lancaster University, Lancaster, United Kingdom
[25]University of Arizona, Tucson, Arizona 85721
[26]Lawrence Berkeley National Laboratory and University of California, Berkeley, California 94720
[27]University of California, Davis, California 95616
[28]California State University, Fresno, California 93740
[29]University of California, Irvine, California 92697
[30]University of California, Riverside, California 92521
[31]Florida State University, Tallahassee, Florida 32306
[32]University of Hawaii, Honolulu, Hawaii 96822
[33]Fermi National Accelerator Laboratory, Batavia, Illinois 60510
[34]University of Illinois at Chicago, Chicago, Illinois 60607
[35]Northern Illinois University, DeKalb, Illinois 60115
[36]Northwestern University, Evanston, Illinois 60208
[37]Indiana University, Bloomington, Indiana 47405
[38]University of Notre Dame, Notre Dame, Indiana 46556
[39]Iowa State University, Ames, Iowa 50011
[40]University of Kansas, Lawrence, Kansas 66045
[41]Kansas State University, Manhattan, Kansas 66506
[42]Louisiana Tech University, Ruston, Louisiana 71272
[43]University of Maryland, College Park, Maryland 20742
[44]Boston University, Boston, Massachusetts 02215
[45]Northeastern University, Boston, Massachusetts 02115
[46]University of Michigan, Ann Arbor, Michigan 48109
[47]Michigan State University, East Lansing, Michigan 48824
[48]University of Nebraska, Lincoln, Nebraska 68588
[49]Columbia University, New York, New York 10027
[50]New York University, New York, New York 10003
[51]University of Rochester, Rochester, New York 14627
[52]State University of New York, Stony Brook, New York 11794
[53]Brookhaven National Laboratory, Upton, New York 11973
[54]Langston University, Langston, Oklahoma 73050
[55]University of Oklahoma, Norman, Oklahoma 73019
[56]Brown University, Providence, Rhode Island 02912
[57]University of Texas, Arlington, Texas 76019
[58]Texas A&M University, College Station, Texas 77843
[59]Rice University, Houston, Texas 77005
[60]University of Washington, Seattle, Washington 98195
(August 29, 2000)

The DØ Collaboration has measured the inclusive jet cross section in $\bar{p}p$ collisions at $\sqrt{s}$ = 630 GeV. The results for pseudorapidities $|\eta| < 0.5$ are combined with our previous results at $\sqrt{s} = 1800$ GeV to form a ratio of cross sections with smaller uncertainties than either individual measurement. Next-to-leading-order QCD predictions show excellent agreement with the measurement at 630 GeV; agreement is also satisfactory for the ratio. Specifically, despite a 10% to 15% difference in the absolute normalization, the dependence of the ratio on jet transverse momentum is very similar for data and theory.

For reactions with large momentum transfers, quantum chromodynamics (QCD) treats complex proton-antiproton interactions in terms of simpler scattering processes involving only one constituent from each particle. Identifying these "parton" constituents with quarks and gluons, perturbative QCD calculates production cross sections for scattered partons (observed as showers or "jets" of collimated particles) that also depend on empirically-determined parton distribution functions (PDF) of the proton.

This measurement compares the production rate of jets as a function of their transverse energy, E_T, at two $\bar{p}p$ center-of-mass energies: $\sqrt{s} = 630$ GeV and 1800 GeV. This comparison reduces the systematic uncertainties and minimizes the prediction's sensitivity to choice of PDF.

In the simple parton model, inclusive jet cross sections scale with $\sqrt{s}$ in the sense that the dimensionless quantity $f(x_T) = E_T^4 \cdot E\frac{d^3\sigma}{d^3p}$, as a function of jet $x_T \equiv \frac{2E_T}{\sqrt{s}}$, does not depend on $\sqrt{s}$ [1]. The ratio of such scaled cross sections for different energies are unity for all x_T. Although previous data [2,3] exhibited significant deviation from this naive scaling, the dimensionless framework provides a useful context for comparison with QCD. The DØ collaboration at the Fermilab Tevatron recently published the inclusive jet cross section at $\sqrt{s} = 1800$ GeV using 95700 ± 500 nb^{-1} of data [4]. This Letter presents our complementary measurement at $\sqrt{s} = 630$ GeV, using a sample of 538 ± 22 nb^{-1} of data [5]. Because the data at both values of $\sqrt{s}$ were collected with the same detector [6], many uncertainties in the results are highly correlated, and the ratio of the cross sections has greater precision than either of the absolute measurements.

The differential jet cross section, $d^2\sigma/dE_T d\eta$, is measured in bins of E_T and pseudorapidity, $\eta \equiv -\ln\left(\tan\frac{\theta}{2}\right)$, where θ is the polar angle of the jet relative to the proton beam. (In this formulation, the dimensionless cross section, averaged over azimuth, is $\frac{E_T^3}{2\pi} \cdot d^2\sigma/dE_T d\eta$.) The DØ reconstruction algorithm defines a jet by the total E_T observed in calorimeter cells contained within a cone of radius $\mathcal{R} \equiv \left[(\Delta\eta)^2 + (\Delta\phi)^2\right]^{\frac{1}{2}} = 0.7$, where ϕ is the azimuthal angle. When two such clusters of cells overlap, they are merged into a single jet if they share more than 50% of the E_T of the lower-E_T cluster; otherwise, they are split into two separate jets, each defined by its own η-ϕ centroid and E_T value [7].

The online trigger requires at least one jet above a set threshold. The offline data selection procedure, which suppresses backgrounds from electrons, photons, noise, and cosmic rays, follows the methods used in the 1800 GeV analysis [8,9]. The efficiency of jet selection is approximately 96% and is nearly independent of jet E_T. To maintain precision in jet E_T, a vertex requirement removes jets resulting from $\bar{p}p$ interactions more than 50 cm from the center of the detector, thereby reducing the total efficiency to 82%. The uncertainty on the cross section associated with all efficiencies is $< 0.5\%$ [9].

Jet energies are corrected [10] for the energy response of the DØ calorimeter to hadrons, the broadening of the hadronic shower, and energy from multiple interactions, calorimeter noise, and the underlying event (fragmentation of the spectator partons). The response correction increases the E_T of jets by 22% for measured calorimeter E_T of 20 GeV, and by 15% for jet E_T above 100 GeV. The 1% showering correction recovers the net energy lost when hadrons from inside the R=0.7 cone deposit energy outside it as they interact within the calorimeter. Calorimeter noise, from electronics and from uranium activity, contributes on average 1.6 GeV of E_T to each jet. The underlying event contributes 0.6 GeV of E_T to each jet at $\sqrt{s} = 630$ GeV, compared to 0.9 GeV at $\sqrt{s} = 1800$ GeV. The corrections offset one another, so that a jet's measured E_T typically increases by 12% to 14% after implementing all energy scale corrections. Uncertainties in the corrections for noise and response dominate the systematic uncertainty of the final result.

Both detector imperfections and random fluctuations in shower development of individual jets within the calorimeter result in the smearing of a jet's E_T about its true value. The finite E_T resolution shifts the observed cross section to higher E_T, especially in the most steeply falling regions of the distribution. The measurement of jet resolution as a function of E_T and the unsmearing procedure follow the steps described in Ref. [4]. The unsmearing correction is larger at 630 GeV than at 1800 GeV because the cross section is significantly steeper at the E_T values of interest.

Figure 1 depicts the inclusive jet cross section at $\sqrt{s} = 630$ GeV in the pseudorapidity bin $|\eta| < 0.5$. Each data point indicates the E_T at which the cross section within that bin has its average value. The bin widths are chosen to match the bins in x_T from the $\sqrt{s} = 1800$ GeV analysis. Table I reports the bin ranges, point positions, and uncertainties. The solid line in Fig. 1 indicates the result of a calculation using the JETRAD next-to-leading-order (NLO) partonic event generator [11] and the CTEQ3M PDFs [12]. The renormalization and factorization scales are set to $\mu = E_T^{\max}/2$, where $E_T^{\max}$ corresponds to the E_T of the leading jet in an event.

Figure 2 compares the cross section to the NLO QCD prediction in greater detail. The "baseline" renormalization and factorization scales are set to $\mu = E_T^{\max}/2$; additional lines in Fig. 2 indicate the predictions that result from changes in either PDF or μ relative to the baseline prediction specified for that pane. The phenomenological parameter $\mathcal{R}_{\text{sep}}$ [7] was set to the conventional value of 1.3 because at this value the predictions reproduce the jet-merging behavior observed in the data. The shaded regions in Fig. 2 indicate the one standard deviation systematic uncertainty of the measurement, and the vertical bars indicate the statistical uncertainty. The first pre-

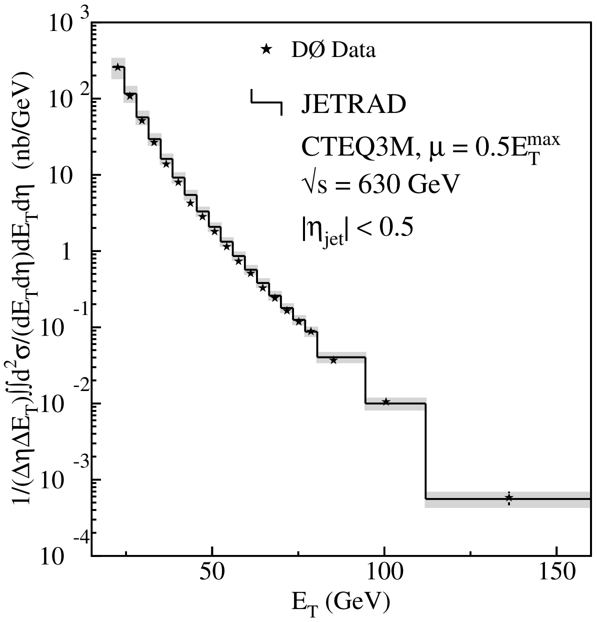

FIG. 1. The inclusive jet cross section at $\sqrt{s} = 630$ GeV, integrated over azimuth and averaged over $|\eta| < 0.5$. The shaded band corresponds to the systematic uncertainties in the measured cross section and the solid line shows a prediction from NLO QCD.

diction, generated with the MRST [13] PDF, is shown to best reproduce the normalization of the data, but the CTEQ4HJ [14] curve in the second pane appears to provide the closest match in shape. Changing μ modifies both the normalization and the shape of the predictions, as seen in the third pane. We quantify the agreement between the data and the various predictions with a χ^2 comparison, as described below.

Combining the cross section information of this Letter with that of Ref. [4], Fig. 3 displays the ratio of dimensionless jet cross sections as a function of x_T. The observed ratio ranges from 1.48 to 1.85, depending on the value of x_T. The largest uncertainties arise from the response and noise corrections, and the remainder consists primarily of resolution and luminosity uncertainties. Although the systematic errors on the individual cross sections range from 10.4% to as much as 30.0%, strong correlations in the measurements reduce the uncertainty on the ratio to values as small as $\pm 5.4\%$. The two final columns of Table I provide the numerical information for the ratio.

As shown in Fig. 3, NLO QCD predictions for the ratio lie systematically above the data throughout most of the measured x_T range, in particular between x_T of 0.1 and 0.2, where the ratio has the smallest statistical uncertainty. Choice of PDF has little effect on the prediction — only the renormalization/factorization scales change the prediction appreciably.

A covariance matrix χ^2 comparing data and theory provides a measure of the probability that the theory

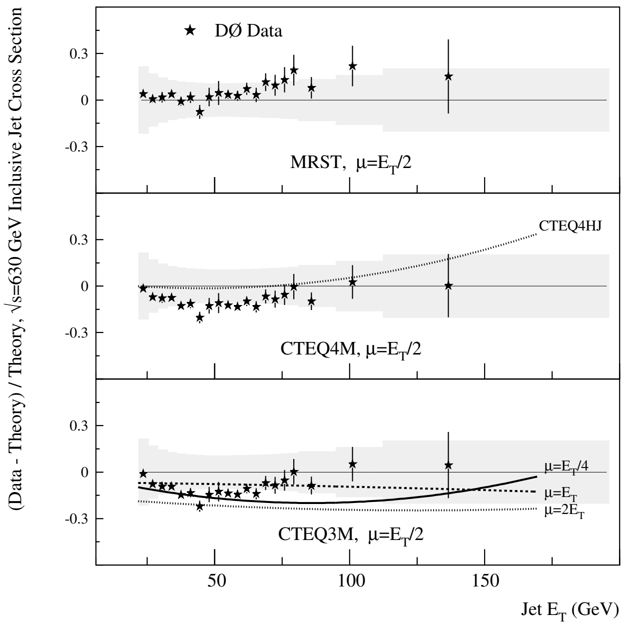

FIG. 2. The inclusive jet cross section at $\sqrt{s} = 630$ GeV compared to several NLO QCD predictions. Error bars indicate statistical uncertainties and shaded bands correspond to systematic uncertainties. The horizontal lines at zero indicate the baseline prediction that is named in each pane; additional lines indicate theoretical variations relative to the baseline.

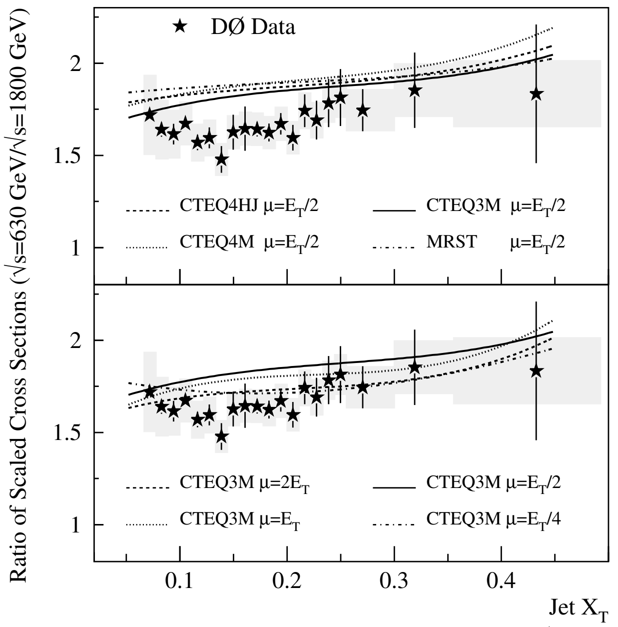

FIG. 3. Ratio of dimensionless jet cross sections (numerator $\sqrt{s} = 630$ GeV, denominator $\sqrt{s} = 1800$ GeV) compared to NLO QCD as given by JETRAD.

Bin E_T (GeV)	Plotted E_T (GeV)	Plotted x_T	Cross Sec. (nb/GeV) $\pm$ Stat. Error	Cross Sec. Sys. Error (%)	Ratio $\pm$ Stat.	Ratio Sys. (%)
21.0 – 24.5	22.6	0.072	$(2.56 \pm 0.03) \times 10^{2}$	21.5	1.72 ± 0.03	12.7
24.5 – 28.0	26.1	0.083	$(1.07 \pm 0.02) \times 10^{2}$	16.9	1.64 ± 0.04	9.7
28.0 – 31.5	29.6	0.094	$(5.14 \pm 0.16) \times 10^{1}$	14.2	1.62 ± 0.06	8.0
31.5 – 35.0	33.1	0.105	$(2.67 \pm 0.05) \times 10^{1}$	12.6	1.67 ± 0.03	7.0
35.0 – 38.5	36.7	0.116	$(1.37 \pm 0.04) \times 10^{1}$	11.6	1.57 ± 0.04	6.3
38.5 – 42.0	40.2	0.127	$(7.96 \pm 0.27) \times 10^{0}$	11.1	1.59 ± 0.06	6.0
42.0 – 45.5	43.7	0.139	$(4.24 \pm 0.20) \times 10^{0}$	10.7	1.48 ± 0.07	5.8
45.5 – 49.0	47.2	0.150	$(2.83 \pm 0.16) \times 10^{0}$	10.5	1.63 ± 0.09	5.5
49.0 – 52.5	50.7	0.161	$(1.81 \pm 0.13) \times 10^{0}$	10.4	1.64 ± 0.12	5.4
52.5 – 56.0	54.2	0.172	$(1.14 \pm 0.03) \times 10^{0}$	10.4	1.64 ± 0.04	5.4
56.0 – 59.5	57.7	0.183	$(7.35 \pm 0.21) \times 10^{-1}$	10.5	1.62 ± 0.05	5.4
59.5 – 63.0	61.2	0.194	$(5.07 \pm 0.17) \times 10^{-1}$	10.7	1.67 ± 0.06	5.4
63.0 – 66.5	64.7	0.205	$(3.29 \pm 0.14) \times 10^{-1}$	10.8	1.60 ± 0.07	5.5
66.5 – 70.0	68.2	0.216	$(2.42 \pm 0.12) \times 10^{-1}$	11.1	1.74 ± 0.09	5.5
70.0 – 73.5	71.7	0.228	$(1.64 \pm 0.10) \times 10^{-1}$	11.3	1.69 ± 0.10	5.6
73.5 – 77.0	75.2	0.239	$(1.18 \pm 0.08) \times 10^{-1}$	11.6	1.78 ± 0.13	5.8
77.0 – 80.5	78.7	0.250	$(8.79 \pm 0.72) \times 10^{-2}$	12.0	1.81 ± 0.15	5.9
80.5 – 94.5	85.2	0.271	$(3.69 \pm 0.23) \times 10^{-2}$	13.2	1.74 ± 0.11	6.4
94.5 – 112.0	100.5	0.319	$(1.05 \pm 0.11) \times 10^{-2}$	15.9	1.85 ± 0.20	7.7
112.0 – 196.0	136.2	0.432	$(5.81 \pm 1.19) \times 10^{-4}$	20.1	1.83 ± 0.38	9.7

TABLE I. Inclusive jet cross section at $\sqrt{s} = 630$ GeV and the ratio of dimensionless cross sections $f^{630}(x_T)/f^{1800}(x_T)$, where $f(x_T) = E_T^4 \cdot E\frac{d^3\sigma}{d^3p}$ and $x_T = 2E_T/\sqrt{s}$. The cross sections are all integrated over azimuth and averaged in the range $|\eta| < 0.5$.

describes the observed results. To verify that our covariance matrix, built mostly from correlated systematic uncertainties, produces results that are consistent with a standard χ^2 distribution with 20 degrees of freedom, we generated 20 million pseudo-experiments using a Monte Carlo program. Each statistical and systematic error was simulated and varied randomly using appropriate correlations in E_T and $\sqrt{s}$. Systematic errors were not always assumed to be Gaussian distributed; some numbers were drawn from flat probability distributions where appropriate. The ensemble of χ^2 comparisons (between the original input and each of the final, randomly-varied distributions) is in excellent agreement with the shape of the χ^2 function for 20 degrees of freedom. We find that the standard probability obtained from an integral of the χ^2 distribution provides an appropriate vehicle for comparing data with predictions.

Table II reports both the χ^2 values and the χ^2 probabilities for the comparison of the data with different NLO QCD predictions. The inclusive jet cross section at $\sqrt{s} = 630$ GeV is consistent with all tested PDF sets and μ scales with only two exceptions. For the ratio of the cross sections, there is no significant difference in shape between data and theory, and essentially all the predictions lie within an acceptable range. The overall results in Table II indicate reasonable agreement between the ratio and NLO QCD.

We performed a second test to quantify the observed difference in the normalization of the ratio, without particular regard to the shapes of the distributions. Using the covariance matrix and assuming that the value of the ratio is a constant with respect to x_T, we found the best-fit horizontal line for the data. The χ^2 value that results from a comparison of this single point to the equivalently-calculated theory point yields the probabilities listed in the final column of Table II. In every case, discarding the information on shape in favor of a comparison of normalization results in poorer agreement between data and the theory, particularly for the often-favored scale of $\mu = E_T^{\max}/2$.

In conclusion, we have measured the inclusive jet cross section at two center-of-mass energies, 630 GeV and 1800 GeV. Both the published data at 1800 GeV [4] and the data presented here at 630 GeV are generally well-described by NLO QCD, with the exception of predictions using CTEQ3M($2E_T^{\max}$) and MRSTGD PDFs. In the ratio of dimensionless cross sections at the two energies, experimental uncertainties are much smaller and differences in the predictions from choice of PDF are less important. NLO predictions for the ratio exhibit satisfactory agreement with the shape of the observed ratio. In terms of only the normalization however, the absolute values of the predictions lie significantly higher than the data, especially for the standard scale $\mu = E_T^{\max}/2$.

We thank the staffs at Fermilab and at collaborating institutions for contributions to this work, and acknowledge support from the Department of Energy and National Science Foundation (USA), Commissariat

PDF	μ	630 GeV C. Sec.		Ratio		Norm.	
		χ^2	Prob.	χ^2	Prob.	χ^2	Prob.
	$2{\cdot}E_T^{\max}$	40.5	0.43%	17.9	59.4%	3.33	6.81%
	E_T	25.9	16.8%	21.6	36.2%	7.13	0.76%
CTEQ3M	$E_T^{\max}/2$	30.4	6.37%	20.5	42.5%	9.56	0.20%
	$E_T^{\max}/4$	27.5	12.2%	15.1	77.4%	1.45	22.93%
CTEQ4M	$E_T^{\max}/2$	24.1	23.8%	22.4	31.9%	10.67	0.11%
CTEQ4HJ	$E_T^{\max}/2$	18.9	52.5%	21.0	40.0%	13.21	0.03%
MRST	$E_T^{\max}/2$	22.6	30.7%	22.2	33.0%	12.60	0.04%
MRSTGU	$E_T^{\max}/2$	14.9	78.2%	19.5	48.7%	11.07	0.09%
MRSTGD	$E_T^{\max}/2$	51.8	0.012%	24.1	23.9%	12.92	0.03%

TABLE II. χ^2 comparisons for the cross section at $\sqrt{s} = 630$ GeV (20 degrees of freedom), the ratio of cross sections (20 degrees of freedom), and a comparison for the ratio involving only the normalization (one degree of freedom).

à L'Energie Atomique and CNRS/Institut National de Physique Nucléaire et de Physique des Particules (France), Ministry for Science and Technology and Ministry for Atomic Energy (Russia), CAPES and CNPq (Brazil), Departments of Atomic Energy and Science and Education (India), Colciencias (Colombia), CONACyT (Mexico), Ministry of Education and KOSEF (Korea), CONICET and UBACyT (Argentina), A.P. Sloan Foundation, and the A. von Humboldt Foundation.

[1] R.P. Feynman, R.D. Field, and G.C. Fox, Phys. Rev. D 18 3320, 1978.
[2] UA2 Collaboration, J.A. Appel *et al.*, Phys. Lett. **B160**, 349 (1985).
[3] CDF Collaboration, F. Abe *et al.*, Phys Rev. Lett. **70**, 1376 (1993).
[4] DØ Collaboration, B. Abbott *et al.*, Phys. Rev. Lett. **82**, 2451 (1999).
[5] J. Krane, J. Bantly, and D. Owen, Fermilab-TM-2000, 1997, (unpublished).
[6] DØ Collaboration, S. Abachi *et al.*, Nucl. Instrum. Methods Phys. Res. A **338**, 185 (1994).
[7] B. Abbott *et al.*, Fermilab-Pub-97-242-E, 1997, (unpublished).
[8] V.D. Elvira, Ph. D. Thesis, Universidad de Buenos Aires, 1995 (unpublished), `http://www-d0.fnal.gov/results/publications_talks/thesis/thesis.html` .
[9] J. Krane, Ph. D. Thesis, University of Nebraska–Lincoln, 1998 (unpublished), `http://fnalpubs.fnal.gov/techpubs/theses.html` .
[10] DØ Collaboration, B. Abbott *et al.*, Nucl. Instrum. Methods Phys. Res. A **424**, 352 (1999).
[11] W.T. Giele, E.W.N. Glover, and D.A. Kosower, Phys. Rev. Lett. **73**, 2019 (1994).
[12] H.L. Lai *et al.*, Phys. Rev. D **51**, 4763 (1995).
[13] A.D. Martin *et al.*, Eur. Phys. J. C 4, 463 (1998).
[14] H.L. Lai *et al.*, Phys. Rev. D **55**, 1280 (1997).